

Some remarks on single- and double-porosity modeling of coupled chemo-hydro-mechanical processes in clays

*Original*

Some remarks on single- and double-porosity modeling of coupled chemo-hydro-mechanical processes in clays / Della Vecchia, Gabriele; Musso, Guido. - In: SOILS AND FOUNDATIONS. - ISSN 0038-0806. - STAMPA. - 56:5(2016), pp. 779-789. [10.1016/j.sandf.2016.08.004]

*Availability:*

This version is available at: 11583/2658369 since: 2016-11-30T17:27:17Z

*Publisher:*

Elsevier

*Published*

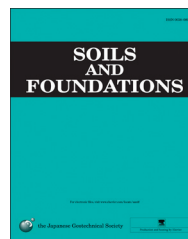
DOI:10.1016/j.sandf.2016.08.004

*Terms of use:*

This article is made available under terms and conditions as specified in the corresponding bibliographic description in the repository

*Publisher copyright*

(Article begins on next page)



IS-Cambridge

# Some remarks on single- and double-porosity modeling of coupled chemo-hydro-mechanical processes in clays

 Gabriele Della Vecchia<sup>a</sup>, Guido Musso<sup>b,\*</sup>
<sup>a</sup>Dipartimento di Ingegneria Civile ed Ambientale, Politecnico di Milano, Piazza Leonardo da Vinci, 32, 20133 Milano, Italy

<sup>b</sup>Dipartimento di Ingegneria Strutturale, Edile e Geotecnica, Politecnico di Torino, Corso Duca degli Abruzzi, 24, 10129 Torino, Italy

Received 29 June 2015; received in revised form 22 January 2016; accepted 7 April 2016

Available online 26 September 2016

## Abstract

Active clays are known to possess an aggregated structure, which justifies the use of double-porosity models to reproduce their behavior. Simulation of chemo-mechanical processes requires instead the introduction of a relevant number of coupled mechanical and transport laws. It follows that double porosity models for coupled chemo-hydro-mechanical require a relevant number of parameters, which are twice those needed by single porosity models. The aim of this work is to evaluate the consequences of using single- and double-porosity frameworks to simulate the transient chemo-mechanical processes in active clays, showing how models based on simple microstructural considerations can help in performing simulations which are a reasonable trade-off between simplicity and accuracy. In particular with single porosity models, it might be necessary introducing parameters having a doubtful meaning to describe adsorption–desorption processes. This type of assumption is not required by double porosity models. While for compacted clays these conclusions are corroborated with microstructural observations, the same hold also when reproducing the behavior of an active clay at a remolded condition. In this latter case the delay of swelling with respect to desalinization, typical of remolded conditions, was satisfactorily reproduced only with double porosity models.

© 2016 The Japanese Geotechnical Society. Production and hosting by Elsevier B.V. This is an open access article under the CC BY-NC-ND license (<http://creativecommons.org/licenses/by-nc-nd/4.0/>).

**Keywords:** Bentonites; Active clays; Coupled processes; Double-porosity models; Single-porosity models; Ionic diffusion

## 1. Introduction

The mineralogy of active clays is characterized by an electrical imbalance which causes, together with the high specific surface, a chemistry-dependent behavior, since forces exchanged at the particle scale are influenced by electro-chemical interactions. Significant macroscopic effects descend: both volume changes and shear strength depend on the chemical composition of the pore fluid (dielectric constant,

electrolyte type and electrolyte concentration). As for conduction processes, active clays behave as semi-permeable membranes, allowing the onset of an osmotic flow (i.e., the flow of water under salt concentration gradients) which is typically not relevant in other types of porous materials. Moreover, the phenomenological response of active clays depends not only on the composition of the constituents, but also on the fabric, which in turn may change with the chemistry of the pore fluid (e.g., Hueckel et al., 1997). In several engineering applications where active clays are of concern, such impermeable barriers for waste disposal or shale formations sustained with different muds during drilling, transport and mechanical processes are coupled. As a consequence of chemically induced fabric changes, both volume and conduction properties evolve during

\*Corresponding author. Fax: +39 011 090 4899.

E-mail addresses: [gabriele.dellavecchia@polimi.it](mailto:gabriele.dellavecchia@polimi.it) (G. Della Vecchia), [guido.musso@polito.it](mailto:guido.musso@polito.it) (G. Musso).

Peer review under responsibility of The Japanese Geotechnical Society.

the transient processes, increasing the complexity of the phenomena and the challenges for engineers.

Different levels of complexities have to be faced, for which justified rational assumptions must be put forward. The first level of complexity concerns the choice of a suitable approach to reproduce the response of the porous medium, i.e., whether adopting a standard equivalent continuum approach would be sufficiently accurate or, if introducing different scales (e.g., through double porosity, double permeability or fractured models) would be relevant. The second level of complexity is related to the number of couplings required to adequately reproduce the investigated processes: coupled fluxes and mutual influence between mechanical and transport processes could be introduced, with the definition of appropriate constitutive laws. The third level of complexity is related to the calibration of the parameters of the adopted model: a relevant number of parameters is normally required and it is not always possible to evaluate all of them through direct measurements.

A standard continuum approach assumes that a single scale is sufficient for reproducing the chemo-hydro-mechanical behavior of the material and thus, just a single set of state variables is introduced. The evaluation of model parameters in this case is solely based on external observations at the macroscopic scale, i.e., the scale of the standard laboratory specimens. In the following, models based on this assumption will be called '*single-porosity models*'. '*Double-porosity models*' assume instead that two scales are relevant. The existence of two scales implies effects on both the hydraulic-transport processes (since mass can be exchanged between the two structural levels) and the mechanical behavior (since the overall observed deformation depends on the mechanical behavior at the two scales and on the interaction between them). Double-porosity models require the definition of two sets of state variables, and thus a higher number of parameters, which can be obtained either through a back analysis of the experimental tests or a direct investigation of the micro-fabric of the material.

The aim of this note is to evaluate the consequences of using single- and double-porosity frameworks to simulate the transient chemo-mechanical processes in active clays, showing how models based on simple microstructural considerations can help in performing simulations which are a reasonable trade-off between simplicity and accuracy.

## 2. Physical processes related to concentration changes and concentration gradients in active clays

Clay particles, due to their small size, crystal structure and platy shape, have very large specific surfaces and are especially influenced by unbalanced force fields at the interface between soil and water. These fields cause interactions between small soil particles, water and dissolved ions, with a significant effect on the hydro-mechanical response of the material (Mitchell and Soga, 2005). For instance, both changes in the chemical concentration of the pore fluid and cation exchange phenomena can induce volumetric strains.

Around a charged colloidal clay particle suspended in a water solution, a double layer develops. Within the double

layer, the concentration of counterions (ions having an electrical charge whose sign is opposite to that of suspended solids) is greater than that of the co-ions (ions having an electrical charge whose sign is the same as that of suspended solids). Within the double layer, the electrical potential is also different from zero. According to the Gouy–Chapman theory, the electrical potential exponentially decreases with the distance from the charged particle. The distance at which the electrical potential is equal to  $1/2.718$  of the value at the solid-to-liquid interface is called the 'thickness' of the double layer,  $\vartheta$ :

$$\vartheta = \sqrt{\frac{\varepsilon_0 \kappa' RT}{2F^2 c_0 z^2}} \quad (1)$$

where  $\varepsilon_0$  is the permittivity of the free space ( $8.85 \times 10^{-12}$  F/m),  $\kappa'$  is the real relative permittivity of the fluid,  $F$  is Faraday's constant ( $9.6485 \times 10^4$  C/mol),  $R$  is the universal gas constant ( $R = 8.314$  J mol $^{-1}$  K $^{-1}$ ),  $T$  is temperature (K),  $c_0$  is the bulk electrolyte concentration (mol/L) and  $z$  is the valence of the ionic species in the solution, supposed to be the same for cations and anions.

The overlapping of double layers causes electrostatic repulsion. The repulsion force  $R_{DL}$  between two platy particles is

$$R_{DL} = 64RTc_0 e^{-\frac{x}{\vartheta}} \quad (2)$$

where  $x$  is the distance between the particles. The same particles are attracted one to the other by the van der Waals attraction force,  $Att$ , as follows:

$$Att = -\frac{A_h}{6\pi x^3} \quad (3)$$

where  $A_h$  is the Hamaker constant, which depends on the compositions of the mineral specie and of the wetting fluid.

According to the DLVO theory (e.g., van Olphen, 1977), the net force exchanged by two parallel platy particles is given by the sum of  $R_{DL}$  and  $Att$  (e.g., Santamarina et al., 2001). The equilibrium between repulsive and attractive forces determines the distance between particles suspended in a fluid having a given dielectric constant and electrolyte concentration. Increasing values of bulk electrolyte concentration lead to smaller values of  $\vartheta$ ; thus,  $R_{DL}$  decreases and so does the distance between particles at equilibrium, and vice versa.

Although the fabric of real soils (both remolded and structured) is very different from that of colloidal suspensions, electrostatic repulsion and van der Waals attraction forces have been combined with total stress and water pressure in a number of formulations to provide a definition of effective stress that is different from that of Terzaghi (e.g., Bolt, 1956; Lambe, 1960). Bolt (1956) and others after him also tried to reproduce the macroscopic volumetric behavior of active monomineral soils exposed to stress and concentration changes starting from the DLVO theory. These models assume that the pores within a saturated soil mass under a given combination of total stress, water pressure and salt concentration have a uniform size.

Clay mineralogy also has important effects on the transport of water mass and charged species. Close to the particle surface, within the range of influence of the electrical field

caused by the electrical imbalance, the movement of co-ions is restricted because of Coulombian repulsion with the solid phase, and the movement of counterions is inhibited by Coulombian attraction. Therefore, the clay acts as a semi-permeable membrane, where the flow of water is possible and the flow of solute is restricted. It also follows that water flows under concentration gradients, which induce osmotic pressure gradients (osmotic flow). Since the electrical interaction vanishes exponentially with the distance from the solid–liquid interface, the restriction to movement of solute within very small pores can be complete, while this effect is less relevant in larger pores.

An osmotic efficiency parameter,  $\omega$ , is then defined, so that the osmotic flow is proportional to the product of the concentration gradients times  $\omega$ , and the electrolyte diffusion is proportional to the concentration gradients times  $(1 - \omega)$ .

Experimental evidence (Bresler, 1973) and models based on thermodynamic concepts (e.g., Dominijanni et al., 2013) show that  $\omega$  is a function of both the concentration in the pore solution and the spacing between particle surfaces.

### 3. Theoretical approaches

In the following, the single-porosity and double-porosity frameworks will be introduced to model the hydro-mechanical response of active clays to chemical solicitations. Both frameworks are based on the solution of water and solute mass balance equations, once given the proper boundary and initial conditions. For each balance equation, proper transport and constitutive laws will be introduced, e.g., the relations linking water flow and solute fluxes to hydraulic and concentration gradients and those linking strain and stress variables. The complete set of balance and constitutive equations is also summed up in Tables 1a and 1b.

For the sake of simplicity, the discussion is limited to saline solutions and one-dimensional conditions, i.e., just volumetric strain is considered. Cation exchange effects will be disregarded.

Throughout the paper, osmotic suction  $\pi$  will be used as the stress-like variable related to the chemical concentration. According to the van Hoff proposal, the relationship between  $\pi$  and molar salt concentration  $c$  in the pore fluid can be expressed as

$$\pi = i c R T \quad (4)$$

with  $i$  being the number of ions into which the salt molecule dissolves in water (e.g.,  $i=2$  for NaCl and  $i=3$  for CaCl<sub>2</sub>).

#### 3.1. Single-porosity models

##### 3.1.1. Chemo-mechanical behavior

In terms of the chemo-mechanical response, the relationship between osmotic suction and volumetric strain is assumed to be reversible. As active clays are more sensitive to chemical effects at low concentrations, the following non-linear

Table 1a

Summary of balance equations and constitutive laws for single-porosity models.

<i>Water phase</i>	
Water mass balance	$v = -\frac{K}{\rho_w g} \nabla(p + \rho_w g z) + \frac{\omega K}{\rho_w g} \nabla(\pi)$
Flow of water phase	$\frac{\partial \rho_w \phi}{\partial t} + \nabla \cdot (\rho_w \mathbf{v}) = 0$
Osmotic efficiency $\omega$ – fitting equation based on Bresler (1973) data ( $A=5.5$ , $B=-1.5$ and $C=-1.3$ )	$\log \omega = B - \arctan[A(\log(10b\sqrt{c}) + C)]$
<i>Solute</i>	
Mass balance of solute	$\frac{\partial c \phi}{\partial t} + \nabla \cdot (\mathbf{j}) + f = 0$
Flux of solute	$\mathbf{j} = c(1 - \omega)\mathbf{v} - D_0 \nabla c$
Adsorption rate	$f = \frac{\partial \rho_s^w q}{\partial t}$
Freundlich adsorption isotherm	${}^w q = \Gamma \cdot c^n$
Effective diffusion parameter	$D_0 = (1 - \omega)D$
<i>Mechanical behavior</i>	
Constitutive law for volume strains upon concentration changes	$d\varepsilon_{vol} = \frac{\kappa}{\pi} d\pi$

stress–strain relation is chosen:

$$d\varepsilon_{vol} = \frac{\kappa}{\pi} d\pi \quad (5)$$

Despite the fact that chemo-plastic effects are known to occur in active clays (e.g., Loret et al., 2002; Guimarães et al., 2013), the irreversibility in the mechanical response is disregarded here in order not to introduce other levels of complexity which could hinder the conclusions drawn in terms of coupling between chemical, hydraulic and mechanical processes.

##### 3.1.2. Water and solute transport

In terms of transport fluxes, both water and solute contributions have to be taken into account. Ignoring electrical and thermal couplings, water mass transport is caused by both hydraulic and concentration gradients, as

$$\mathbf{v} = -\frac{K}{\rho_w g} \nabla(p + \rho_w g z) + \frac{\omega K}{\rho_w g} \nabla(\pi) \quad (6)$$

where  $\mathbf{v}$  is the water seepage velocity,  $K$  is the water hydraulic conductivity,  $p$  is the water pressure,  $\rho_w$  is the water density,  $g$  is the gravitational acceleration and  $z$  is the elevation head. Osmotic efficiency parameter  $\omega$  quantifies the efficiency of the clay as a semipermeable membrane, allowing water to flow with immobile solute ions. Osmotic efficiency is usually assumed to vary between 0 (null efficiency) and 1 (full efficiency) (Lu et al., 2004).

The first term on the right side of Eq. (6) represents the direct flow component, while the second term is the coupled one, i.e., the osmotic flow. The transport of the solute mass is given by flux  $\mathbf{j}$ , which can be split into the sum of an advective term (the first one) and a diffusive term (the second one), as follows:

$$\mathbf{j} = c(1 - \omega)\mathbf{v} - D_0 \nabla c \quad (7)$$

where effective diffusion parameter  $D_0$  accounts for membrane effects:

$$D_0 = (1 - \omega)D \quad (8)$$

with  $D$  being the diffusion coefficient in the porous medium, accounting for molecular diffusion, porosity and tortuosity. Dispersion accounts for the direct flow of the salt mass, and thus, is related to chemical concentration gradients, while advection represents the movement of the salt mass due to the flowing water.

### 3.1.3. Mass balance of water and solute

Transport equations are needed to solve the field mass balance equations, which for water and solute, respectively, read as follows:

$$\frac{\partial \rho_w \phi}{\partial t} + \nabla \cdot (\rho_w \mathbf{v}) = 0 \quad (9a)$$

$$\frac{\partial c \phi}{\partial t} + \nabla \cdot (\mathbf{j}) + f = 0 \quad (9b)$$

where  $\phi$  is the porosity (volume of voids over the total volume of the porous medium, whose variation is univocally related to volumetric strain) and  $f$  is the net rate of the transfer of the mass of solute from the liquid phase towards the solid phase. Defining  ${}^wq$  as the mass fraction of the chemical species adsorbed on the solid phase (solid concentration) allows for the rewriting of Eq. (9b) as

$$\frac{\partial c \phi}{\partial t} + \nabla \cdot (\mathbf{j}) + \frac{\partial \rho_d {}^wq}{\partial t} = 0 \quad (10)$$

where  $\rho_d$  is the dry density, i.e., the product of the bulk density of the solid phase,  $\rho_b$ , and the volumetric fraction of solids. Reversible and instantaneous sorption of the solutes is generally assumed. In the following, adsorption/desorption processes are simulated with Freundlich-like isotherms. This approach ignores the mechanisms affecting the mass transfer into the inter-particle and inter-layer pore spaces, where the majority of sorption occurs, as well as the competition for sorption sites. Thus, the concentration of salt adsorbed onto the

solid matrix is written as

$${}^wq = \Gamma \cdot c^n \quad (11)$$

where  $n=1$  implies linear adsorption. The problem is then closed under the assumption of incompressible solid phase and infinitesimal strains by imposing  $d\epsilon_{vol} = -d\phi$ .

### 3.2. Double-porosity model

Despite its success in explaining some features of the observed volumetric response, such as volume decrease upon salinisation, the uniform pore size assumption appears to be controversial when considering the behavior of structured soils (Musso et al., 2013a).

Details concerning the double-porosity formulation can be found in Musso et al. (2013a) and in Musso and Della Vecchia (2015). In the following, the fundamental equations of the model are briefly recalled to allow the comparison between the single- and the double-porosity frameworks. A double-porosity model relies on the existence of a micro-structural and a macro-structural domain. In the case of compacted soils, the micro-structural domain is represented by the space within the soil aggregates, while the macro-structural domain is represented by the space between the aggregates. The global void ratio,  $e$ , can be split into two components, namely, *micro-structural* void ratio  $e_m$  and *macro-structural* void ratio  $e_M$ :

$$e = e_m + e_M = \frac{V_{vm}}{V_s} + \frac{V_{vM}}{V_s}, \quad (12)$$

where  $V_{vm}$  is the volume occupied by the micro-voids,  $V_{vM}$  is the volume occupied by the macro-voids and  $V_s$  is the volume of solids. The micro-structural and macro-structural domains are treated as overlapping and communicating continua, so different pressures and concentrations can be defined in each

Table 1b

Summary of balance equations and constitutive laws for double-porosity models ( $l_m$  is micro,  $l_M$  is macro).

#### Water phase

Water mass balance

Flow of water phase

Exchange term between micro and macro

Osmotic efficiency  $\omega$  – fitting equation based on Bresler (1973) data ( $A=5.5$ ,  $B=-1.5$  and  $C=-1.3$ )

#### Solute

Mass balance of solute

Flux of solute

Exchange term between micro and macro

Effective diffusion parameter

#### Mechanical behavior

Constitutive law for volume strains upon concentration changes

$$\begin{aligned} \frac{\partial \rho_w \phi_m}{\partial t} - q_w^{EX} &= 0 \\ \frac{\partial \rho_w \phi_M}{\partial t} + \nabla \cdot (\rho_w \mathbf{v}) + q_w^{EX} &= 0 \\ \mathbf{v}_m &= \mathbf{0} \\ \mathbf{v}_M &= -\frac{K_M}{\rho_w g} \nabla (p_M + \rho_w g z) + \frac{\omega K_M}{\rho_w g} \nabla (\pi_M) \\ q_w^{EX} &= \frac{q_s^{EX}}{c_m} - \frac{\phi_m}{c_m} \frac{\partial c_m}{\partial t} \\ \log \omega &= B - \arctan[A(\log(10b\sqrt{c}) + C)] \end{aligned}$$

$$\begin{aligned} \frac{\partial c_m \phi_m}{\partial t} - q_s^{EX} &= 0 \\ \frac{\partial c_M \phi_M}{\partial t} + \nabla \cdot (\mathbf{j}) + q_s^{EX} &= 0 \\ \mathbf{j}_m &= \mathbf{0} \\ \mathbf{j}_M &= c_M(1-\omega)\mathbf{v} - D_{M0}\nabla(c_M) \\ q_s^{EX} &= \chi(c_M - c_m) = \tilde{\alpha} \exp(-\tilde{\gamma} c_M) \cdot (c_M - c_m) \\ D_0 &= (1-\omega)D \end{aligned}$$

$$\begin{aligned} d\epsilon_{vol} &= d\bar{\epsilon}_{vol}^M + \alpha^* d\epsilon_{vol}^m \\ d\epsilon_{vol}^m &= \beta e^{-\alpha \pi_m} d\pi_m \\ d\bar{\epsilon}_{vol}^M &= \frac{\bar{\epsilon}_M}{\pi_M} d\pi_M \end{aligned}$$



of them. Micro-porosity  $\phi_m$  is the volume occupied by micro-pores over the total volume, while macro-porosity  $\phi_M$  is the volume occupied by the macro-pores over the total volume, namely,

$$\phi_m = \frac{e_m}{1+e}, \quad \phi_M = \frac{e_M}{1+e} \quad (13)$$

### 3.2.1. Chemo-mechanical behavior

As for the description of the chemo-mechanical behavior, the overall incremental volumetric deformation of the soil,  $d\epsilon_{vol}$ , can be numerically estimated considering separate contributions from macro-structure  $d\bar{\epsilon}_{vol}^M$  and micro-structure  $d\epsilon_{vol}^m$ . Hence,

$$d\epsilon_{vol} = d\bar{\epsilon}_{vol}^M + \alpha^* d\epsilon_{vol}^m \quad (14)$$

where  $d\epsilon_{vol}^m$  is the volumetric microscopic strain and  $d\bar{\epsilon}_{vol}^M$  is defined as the volumetric strain experienced by the macro-structure at a constant aggregate size. Macroscopic and microscopic strains are summed by introducing a coefficient  $\alpha^*$  (being  $0 \leq \alpha^* \leq 1$ ) to take into account the fraction of microstructural strain contributing to the overall deformation of the porous medium, i.e., the part which can be measured from an external observer, according to the framework proposed by Gens and Alonso (1992). The coefficient  $(1 - \alpha^*)$  represents the fraction of microscopic swelling strain that invades the macro-pores. Strain increments are related to the changes in osmotic suction through the mechanical constitutive relations.

$$d\epsilon_{vol}^m = \beta e^{-\alpha\pi_m} d\pi_m \quad (15a)$$

$$d\bar{\epsilon}_{vol}^M = \frac{\bar{\kappa}_\pi}{\pi_M} d\pi_M \quad (15b)$$

where  $\alpha$ ,  $\beta$  and  $\bar{\kappa}_\pi$  are the constitutive material parameters to be calibrated according to the experimental data. It must be noted here that Eq. (15a) (Alonso et al., 1994) is actually a heuristic expression which can appropriately reproduce the prediction of the DLVO theory; it is in accordance with the Mercury Intrusion Porosimetry data presented in Musso et al. (2013a). Eqs. (15a) and (15b) allow for the estimation of the variation in porosity of the two structural domains.

### 3.2.2. Water and solute transport

It is assumed here that significant water and species fluxes occur only through macro-pores. Thus, the micro-porosity domain behaves like ‘dead end pores’, i.e., it is accessible only through transfer from and to the macro-porosity domain. As a consequence,

$$\mathbf{v}_m = \mathbf{0} \quad (16a)$$

$$\mathbf{j}_m = \mathbf{0} \quad (16b)$$

with  $\mathbf{v}_m$  and  $\mathbf{j}_m$  being the flow of water and the flux of salt in the micro-pores.

Transport equations have similar expressions to Eqs. (6) and (7); the flow of water  $\mathbf{v}_M$  and the flux of solute  $\mathbf{j}_M$  in the macro-

pores can be expressed as

$$\mathbf{v}_M = -\frac{K_M}{\rho_w g} \nabla(p_M + \rho_w g z) + \frac{\omega K_M}{\rho_w g} \nabla(\pi_M) \quad (17a)$$

$$\mathbf{j}_M = c_M(1-\omega)\mathbf{v}_M - D_{M0}\nabla(c_M) \quad (17b)$$

where subscript  $M$  is used for variables that refer to the macro-structure. Thus, both  $K_M$  (hydraulic conductivity) and  $D_{M0}$  (effective diffusion) are defined just for the macroscopic domain:

$$D_{M0} = (1-\omega)D_M \quad (18)$$

### 3.2.3. Mass balance of water and solute

The exchange of both water and solute is allowed between the two overlapping continua, so the water mass balance equations in the micro- and macro-porosity domains can be written as

$$\frac{\partial \rho_w \phi_m}{\partial t} - q_w^{EX} = 0 \quad (19a)$$

$$\frac{\partial \rho_w \phi_M}{\partial t} + \nabla \cdot (\rho_w \mathbf{v}_M) + q_w^{EX} = 0 \quad (19b)$$

where  $q_w^{EX}$  is the water mass exchange term between the micro-porosity and the macro-porosity. The similar mass balance of the solute in the two domains reads

$$\frac{\partial c_m \phi_m}{\partial t} - q_s^{EX} = 0 \quad (20a)$$

$$\frac{\partial c_M \phi_M}{\partial t} + \nabla \cdot (\mathbf{j}_M) + q_s^{EX} = 0 \quad (20b)$$

where  $q_s^{EX}$  is the salt mass exchange term. It can be demonstrated that  $q_s^{EX}$  and  $q_w^{EX}$  correlate to each other (Musso et al., 2013a), as follows:

$$q_w^{EX} = \frac{q_s^{EX}}{c_m} - \frac{\phi_m}{c_m} \frac{\partial c_m}{\partial t} \quad (21)$$

The mass exchange is assumed to be proportional to the difference in potential (pressure or saline concentration) between the two domains, by means of first order transfer parameter  $\chi$  (Gerke and van Genuchten, 1993). In this model, it is assumed that the exchange of mass between domains is easier at an increasing aggregate size, as discussed from the micromechanical point of view in Gerke and van Genuchten (1993). Thus, the mass exchange is reproduced by introducing coefficients  $\hat{\alpha}$  and  $\hat{\gamma}$ .

$$q_s^{EX} = \chi(c_M - c_m) = \hat{\alpha} \exp(-\hat{\gamma} c_M) \cdot (c_M - c_m) \quad (22)$$

The higher the ion concentration in macro-pores  $c_M$ , the lower the porosity of the aggregates, thus reducing the possibility of mass exchange between micro- and macro-pores. Vice versa, a reduction in ion concentration implies a higher aggregate porosity, and thus, an easier mass exchange. The problem is then closed imposing that  $d\epsilon_{vol}^m = -d\phi$  and  $d\epsilon_{vol}^M = -d\phi_m$ .

## 4. Model performance

### 4.1. Comparison of model performance: compacted clay

The numerical solutions of the field balance equations for the two approaches – Eqs. (9a) and (9b) for the single-porosity model and Eqs. (19a), (19b), (20a) and (20b) for the double-porosity model – have been obtained via the Finite Element Method using Comsol MultiPhysics<sup>®</sup>, a commercial software particularly suitable for solving strongly coupled problems. A comparison of the predictions of the single- and double-porosity models is presented with reference to a benchmark oedometer test performed on a compacted clay sample of FEBEX bentonite. FEBEX is a natural mixed bentonite proposed as an engineered barrier for radioactive waste disposal (ENRESA, 2000), with abundant active minerals (Montmorillonite fraction  $90 \pm 3\%$ ). Its Cation Exchange Capacity is 102 meq/100 g, liquid limit is  $w_L=102\%$  and plastic limit is  $w_P=53\%$ . A 10.5-mm-thick sample was prepared by statically compacting in oedometer conditions the bentonite powder at its hygroscopic water content ( $w=12\%$ , at a relative humidity of 50%) to the initial dry density  $\rho_d=1.65 \text{ Mg/m}^3$  (void ratio  $e=0.64$ , degree of saturation  $S_r=51\%$ ), then unloading it and finally re-loading it to a total vertical stress  $\sigma=200 \text{ kPa}$ . The ends of the sample were connected to two different reservoirs (see Fig. 1 for a schematic of the testing conditions). A NaCl solution ( $c=5.5 \text{ mol/l}$ ) was poured into the two reservoirs, filling them and saturating the sample, which swelled upon hydration. Once that swelling ceased, the saline solution in the bottom reservoir was removed and substituted with distilled water (renewed daily in order to ensure constant concentration). While the transport of salt occurred from the specimen towards the bottom reservoir, the concentration of salt in the top reservoir was monitored daily by means of electrical conductivity measurements. Sample desalinization caused further delayed

swelling. Once that complete desalinization of the top reservoir was achieved and displacements had ceased, the process was reverted by pouring once again the saline solution into the bottom reservoir. This caused sample shrinkage and the re-salinization of the top reservoir.

Values of hydraulic conductivity (introduced as  $K$  in the single-porosity model and  $K_M$  in the double-porosity model) and chemo-mechanical compliance  $\kappa_\pi$  were taken from the literature (Castellanos et al., 2008). Osmotic efficiency parameter  $\omega$  was evaluated through a relationship from the literature (Bresler, 1973), while the diffusion parameter ( $D$  or  $D_M$ ) was obtained by rescaling the diffusion parameter of NaCl in pure water through a coefficient which depends on porosity (Bourg et al., 2006).

#### 4.1.1. Calibration of parameters for single-porosity model

The single-porosity model is formulated assuming that the ‘immobile’ water within the aggregates is tightly attracted to the solid phase, to such an extent that it is considered as belonging to the solid phase. The ‘solid phase’ would be given here by the aggregates themselves, thus including the presence of water within the microstructure. To ensure consistency with the physics of the problem (and thus, with the double-porosity frame), the bulk density  $\rho_b$  of the equivalent ‘solid phase’ is considered to depend also on the volumetric deformation of the aggregates/clusters:

$$\rho_b = \frac{\rho_s \cdot (1 - (\phi_M + \phi_m)) + \rho_w \cdot \phi_m}{1 - \phi_M} \quad (23)$$

Since micro-porosity would not be defined in a single-porosity model, a constant value of  $\phi_m$  was introduced in Eq. (10), neglecting any further evolution due to changes in chemical composition of pore water. In the simulations presented here, a constant value of  $\phi_m=0.1$  has been used. Parameter  $\Gamma$  was chosen for the linear isotherm on the basis of diffusion data on FEBEX bentonite by García-Gutiérrez et al. (2004) at relevant sample density. Those authors found that the

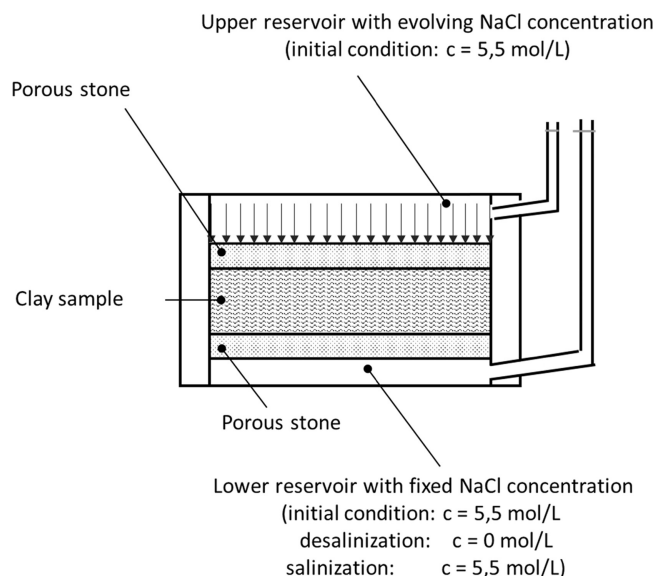


Fig. 1. Scheme of the test conditions for the FEBEX bentonite (Musso et al., 2013a).

Table 2

Hydro-chemo mechanical parameters of the double-porosity and the single-porosity models used for compacted FEBEX bentonite.

Parameters common to both models

Hydraulic conductivity $K$ or $K_M$	$5 \times 10^{-12} \text{ m s}^{-1}$
Diffusion coefficient $D$ or $D_M$	$9 \times 10^{-11} \text{ m}^2 \text{ s}^{-1}$

Parameters of the single-porosity model

Single-porosity compressibility	$\kappa_\pi=0.043$
Constant of the linear isotherm	$\Gamma=1 \times 10^{-3} \text{ m}^3/\text{kg}$
Constant of the Freundlinch isotherm	$\Gamma_F=0.4 \text{ m}^3/\text{kg}$
Exponent of the Freundlinch isotherm	$n=0.4$

Parameters of the double-porosity model

Microstructure compressibility	$\alpha=2 \times 10^{-4} \text{ kPa}^{-1}$	$\beta=3.2 \times 10^{-5} \text{ kPa}^{-1}$
Macrostructure compressibility	$\bar{\kappa}_\pi=0.015$	
Diffraction function	$\alpha^*=0.45$	
Transfer function	$\hat{\alpha}=0.8 \text{ s}^{-1}$	$\hat{\gamma}=8.1 \text{ mol}^{-1}$

experimental data on the diffusion of the  $^{36}\text{Cl}$ - isotope were satisfactorily fitted by adopting an apparent diffusion coefficient  $D_a = 3.4 \times 10^{-11} \text{ m}^2/\text{s}$ . An estimate of  $\Gamma$ , in the case of the linear isotherm, can be performed considering that the apparent diffusion coefficient accounts for both diffusion and adsorption, namely,

$$D_a = \frac{D}{a} \quad (24)$$

where  $a = \phi + \rho_d \Gamma$  is a capacity factor accounting for the capacity of the soil to retard the movement of solute through adsorption. The parameters of the non-linear isotherms were obtained through a back analysis of the test simulated herein.

#### 4.1.2. Calibration of parameters for double-porosity model

Duplicate FEBEX samples, identical to those of the benchmark test, were saturated with different saline  $\text{NaCl}$  and  $\text{CaCl}_2$  solutions in oedometer conditions at constant total vertical stress, and their microstructure was characterized through Mercury Intrusion Porosimetry (MIP) tests. MIP tests allowed for the estimation of microscopic void ratio  $e_m$  and macroscopic void ratio  $e_M$ , for each solute concentration, according to a procedure formerly proposed for unsaturated soils (Romero et al., 2011; Della Vecchia et al., 2013). Detailed descriptions of the procedure and the Pore Size Density diagrams are available elsewhere (Musso et al., 2013a, 2013b). Microscopic void ratio data were converted into microscopic strains (Eq. 13) used to calibrate parameters  $\alpha$  and  $\beta$  of the constitutive equation for the mechanical behavior of the microporosity (Eq. 15a). A comparison between the experimental data and the optimized model predictions is presented in Fig. 2.

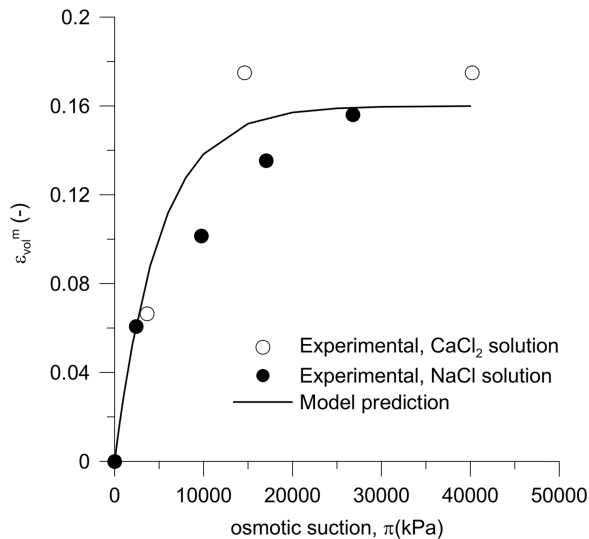


Fig. 2. FEBEX bentonite: Microstructural volume strains at different osmotic suctions as identified on basis of MIP tests and prediction the constitutive model for the microstructure with  $\alpha = 2 \times 10^{-4} \text{ kPa}^{-1}$  and  $\beta = 3.2 \times 10^{-5} \text{ kPa}^{-1}$ .

#### 4.1.3. Comparison of predictions for single-porosity and double-porosity models

The simulations were run with the parameters reviewed in Table 2. Model predictions in terms of the time evolution of the concentration in the top reservoir and displacements are shown in Figs. 3 and 4, respectively. The predicted time evolution of the concentration in the free reservoir (Fig. 3), obtained using the linear adsorption isotherm calibrated in the literature data ( $\Gamma = 1 \times 10^{-3} \text{ m}^3/\text{kg}$  and  $n = 1$ ), is quite satisfactory along the salinization path. However, the rate of dilution is significantly overestimated; after 50 days from the beginning of the desalinization, the measured concentration was around 140 g/l compared to a prediction of about 38 g/l. Since strains are related to the variation in osmotic suction, which in turn is linearly dependent on the concentration, it is not surprising that the chemical consolidation is satisfactorily reproduced, while the swelling is not (Fig. 4). Non-linear Freundlich adsorption was considered as an alternative for obtaining a better reproduction of the desalinization path. In this case, parameters  $\Gamma$  and  $n$  were determined on the basis of a back analysis on the displacement and concentration data. Adopting  $\Gamma = 0.4 \text{ m}^3/\text{kg}$  and  $n = 0.4$  significantly improves the prediction of the evolution of the concentration upon desalinization, while the prediction of salinization gets worse. The displacement prediction is not that satisfactory; in fact, the model is not able to reproduce the discontinuous rate of the evolution of displacements, the latter being a peculiarity of the response of compacted clays that seems to be reproduced only with a double-porosity mechanical model. The double-porosity model allows for both the overall concentration and the displacement response to be reproduced.

#### 4.2. Comparison of model performances: reconstituted clay

A comparison between the predictions of the single- and double-porosity model is presented with reference to the oedometer tests performed by Di Maio (1996) on samples of reconstituted Ponza clay. Ponza clay is a natural bentonite with an 80% clay fraction, mostly composed of sodium montmorillonite, and a plasticity index of 320%. Reconstituted specimens were prepared by mixing powdered clay with distilled water at about the liquid limit. The tests were performed on 20-mm-thick specimens, which were first consolidated to different axial stresses, then exposed to various saturated solutions, namely,  $\text{NaCl}$ ,  $\text{KCl}$  and  $\text{CaCl}_2$ , and finally exposed to distilled water again. The experimental data on two  $\text{NaCl}$  salinization/desalinization tests performed at the vertical stress of 40 and 160 kPa are introduced here for comparison purposes. Note that in these tests the same concentrations (saturated  $\text{NaCl}$  solution and then distilled water) were imposed at the same time at both ends of the specimen (Fig. 5). The parameters used in the simulations are presented in Table 3.

The effective diffusion coefficient ( $D_M$  for the double-porosity model and  $D$  for the single-porosity one) was set to be equal to  $7.05 \times 10^{-10} \text{ m}^2/\text{s}$  on the basis of porosity and free solution diffusion values (Bourg et al., 2006), while a value of  $8 \times 10^{-13} \text{ m/s}$  was chosen for the hydraulic conductivity ( $K_M$  or



Table 3

Hydro-chemo mechanical parameters of the double-porosity and the single-porosity model used for reconstituted Ponza bentonite.

Parameters common to both models		
Hydraulic conductivity $K$ or $K_M$	$8 \times 10^{-13} \text{ m s}^{-1}$	
Diffusion coefficient $D$ or $D_M$	$7 \times 10^{-10} \text{ m}^2 \text{ s}^{-1}$	
Parameters of the single-porosity model		
Single-porosity compressibility	$\kappa_\pi=0.265$ ( $\sigma_v=40 \text{ k Pa}$ ) or $0.158$ ( $\sigma_v=160 \text{ k Pa}$ )	
Constant of the linear isotherm	$\Gamma=1 \text{ m}^3/\text{kg}$ and $2 \text{ m}^3/\text{kg}$	
Constant of the Freundlinch isotherm	$\Gamma_F=40 \text{ m}^3/\text{kg}$	
Exponent of the Freundlinch isotherm	$n=0.4$	
Parameters of the double-porosity model		
Microstructure compressibility ( $\sigma_v=40 \text{ k Pa}$ )	$\alpha=4 \times 10^{-4} \text{ k Pa}^{-1}$	$\beta=1.0 \times 10^{-3} \text{ k Pa}^{-1}$
Microstructure compressibility ( $\sigma_v=160 \text{ k Pa}$ )	$\alpha=4 \times 10^{-4} \text{ k Pa}^{-1}$	$\beta=1.6 \times 10^{-3} \text{ k Pa}^{-1}$
Macrostructure compressibility	$\bar{\kappa}_\pi=0$	
Interaction function	$\alpha^*=1$	
Transfer function	$\hat{\alpha}=1 \text{ s}^{-1}$	$\hat{\gamma}=1 \text{ mol}^{-1}$

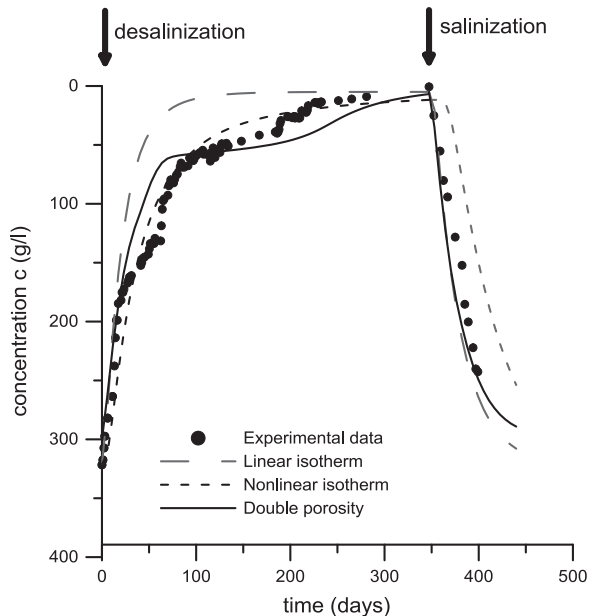


Fig. 3. FEBEX bentonite test: History of NaCl concentration in top (free) reservoir.

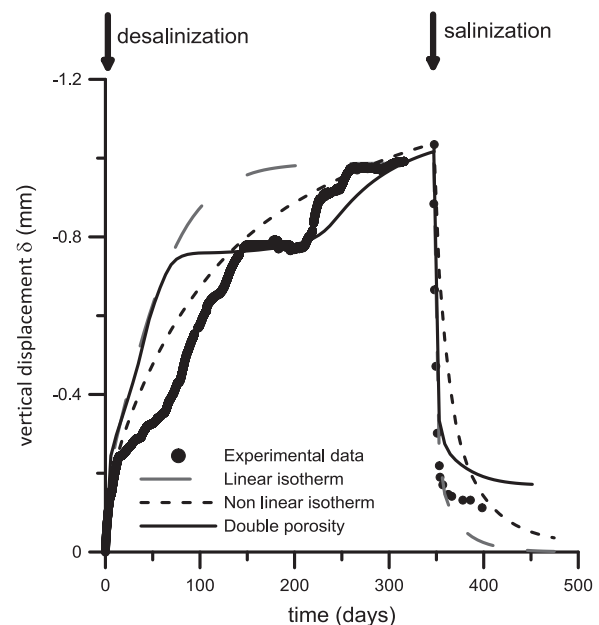


Fig. 4. FEBEX bentonite test: Displacement time evolution.

$K$ ). The osmotic efficiency was also assumed to vary with the concentration in this case (Bresler, 1973). The single-porosity model is formulated under the same assumptions as those used for compacted clays, the value of  $\kappa_\pi$  being calibrated directly in the experimental test analyzed. The consequences of introducing linear and non-linear adsorption isotherms were studied. The parameters of the Freundlich isotherms, which influence the temporal evolution of strains, were imposed for a sensitivity analysis.

These tests were also simulated by means of the double-porosity model. When the double-porosity framework is applied to reconstituted clays, the role of the fundamental microstructural units is taken by clusters of clay particles, saturated by immobile inter-layer water and external adsorbed water (Hueckel et al., 1997). The deformation of the sample is

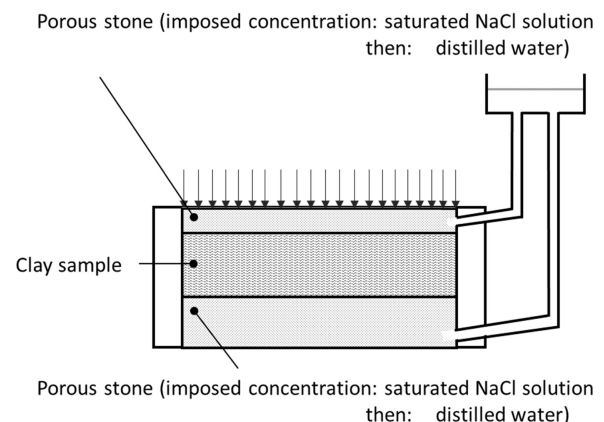


Fig. 5. Test conditions for the Ponza bentonite (Di Maio, 1996).

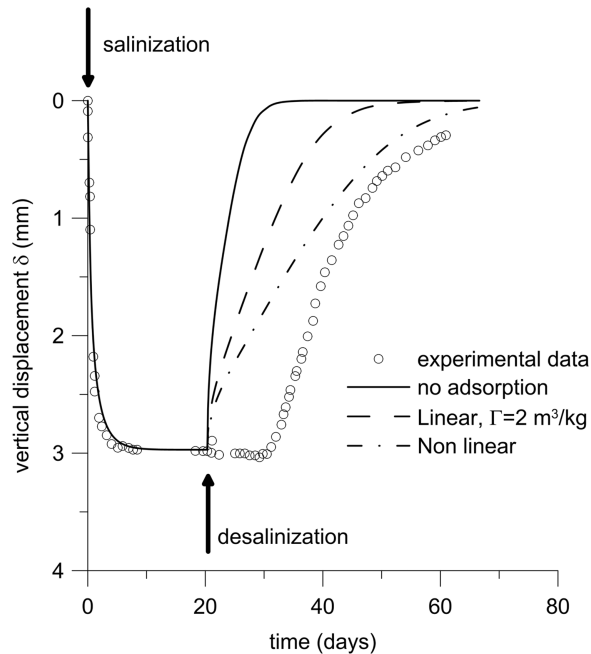


Fig. 6. Ponza bentonite test: History of displacements during salinization/desalinization. Single-porosity model predictions.

assumed here to be equal to the deformation of the microstructure, i.e.,  $\kappa_\pi=0$ , and the invasion of the microstructure into the macro-voids is inhibited (i.e.,  $\alpha^*=0$ ). The compliance parameters of the microstructure ( $\alpha$  and  $\beta$ ) were calibrated for each path on the basis of the final displacement of the samples subjected to cycles of salinization/desalinization, while the exchange parameters were calibrated for the entire set of available tests in order to satisfactorily reproduce the displacement history.

Single-porosity model predictions, for the displacement evolution in the sample subjected to salinization/desalinization at vertical stress 40 kPa are shown in Fig. 6. The predictive capability of the model without adsorption is satisfactory during the salinization stage, but the rate of swelling is vastly overestimated during desalinization. Even when introducing linear or non-linear Freundlich isotherms, it is not possible to satisfactorily reproduce the swelling history; more noticeable is the significant delay between the start of the desalinization (indicated by the black arrow in Fig. 6) and the beginning of sample swelling.

The peculiar delayed response of the reconstituted clays with desalinization can vice versa be well reproduced by means of the double-porosity model, as shown in Fig. 7, for the samples loaded up to 40 and 160 kPa. The delay between desalinization and the occurrence of displacements is strongly related to the assumption of ignoring the macro-pore deformation, which would have commenced immediately after desalinization. As the vertical displacement is related just to the micro-pore deformation, the time delay is essentially ruled by the solute mass transfer between the two domains, and thus, by the shape of the exchange function (Eq. 22). All the transport parameters for both simulations are kept the same, except for the compressibility of the microstructure, which is different for each path to empirically account for

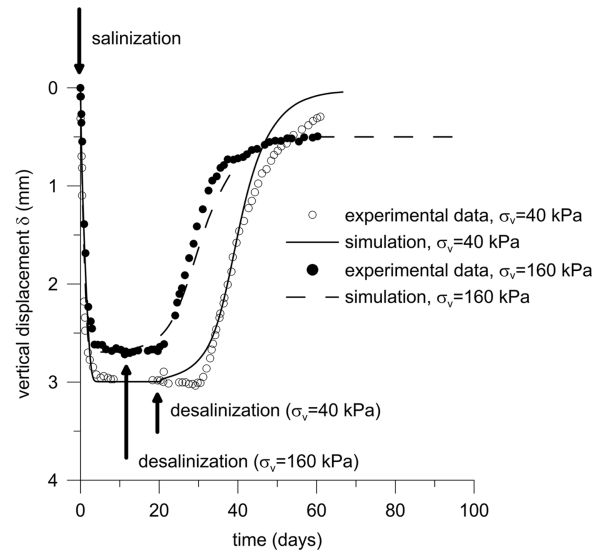


Fig. 7. Ponza bentonite test: History of displacements during salinization/desalinization. Double-porosity model predictions.

the chemo-plasticity effects. Moreover, the overall displacement response is conveniently reproduced in this case by the double-porosity models, once the approach is suitably modified to account for the difference in microstructure between reconstituted and compacted clays.

## 5. Discussion and final remarks

Coupled chemo-hydro-mechanical double-porosity models for structured active materials require careful calibration and implementation; thus, single-porosity models can be thought of as an alternative. To be used in such a context, in the formulation of the latter, it is necessary to assign a weak meaning to 'adsorption', in order to indicate not only the process of the attachment of chemical species to the solid phase, but also their migration from the macro-pores towards the micro-pores. The 'adsorption' term must then somehow also incorporate the effects of the exchange rate between the micro- and the macro-porosity (van Genuchten and Clearly, 1982; Brusseau et al., 1994)). Figs. 3 and 4 show that, if the parameter calibration of the linear adsorption isotherm is performed by fitting the desalinization data, the predictions of the salinization path are not even satisfactory in terms of the concentration history. One possibility for improving the predictive capabilities of the single-porosity model would be the introduction of hysteresis in terms of adsorption isotherms, i.e., using different parameters along sorption and desorption paths. For the case of FEBEX Bentonite, an excellent prediction is achieved by adopting non-linear desorption ( $\Gamma=0.4 \text{ m}^3/\text{kg}$ ,  $n=0.4$ ) and linear sorption ( $\Gamma=1 \cdot 10^{-3} \text{ m}^3/\text{kg}$ ,  $n=1$ ). Despite the good phenomenological prediction, it is worth checking the implications of this strategy in terms of the relationship between solute and adsorbed concentration, as shown in Fig. 8. The adsorbed salt predicted by the non-linear isotherm for the maximum solute concentration (i.e., 4 g per 1 g of solid grains) is physically unreasonable. As a further point, when history dependence is introduced into the adsorption models, it is

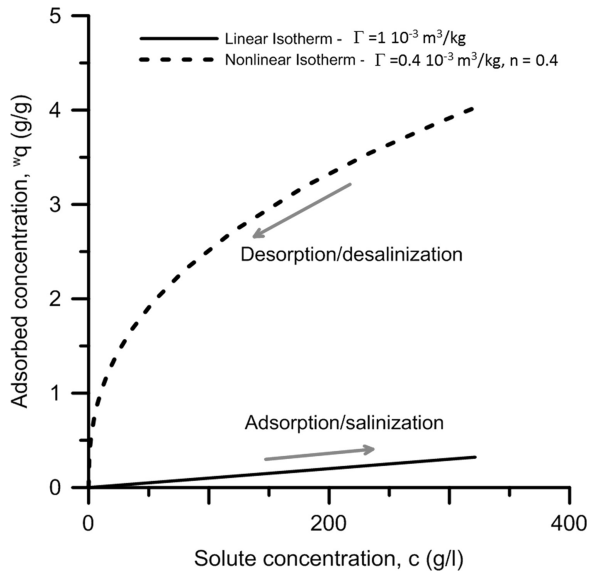


Fig. 8. Comparison of adsorption isotherms used in the simulations of FEBEX bentonite test.

necessary to check the consistency. At the boundaries of the time-domain investigated here, the following constraint has to be satisfied (van Genuchten and Cleary, 1982):

$${}^w q = \Gamma_a \cdot c_M^{n_a} = \Gamma_d \cdot c_M^{n_d} \quad (25)$$

where subscript *a* indicates adsorption and subscript *d* indicates desorption. According to Eq. (25), at the end of a salinization–desalinization cycle, the concentration should be equal to the initial one. As shown in Fig. 8, this condition is not satisfied by the best-fitting parameters used for the simulation of the measured displacement/concentration. The numerical analyses presented in this study would then indicate that the overall macroscopic simulation of the coupled transport and mechanical processes is possible, but not recommended, since it can require the adoption of non-physical parameters describing adsorption–desorption.

On the contrary, the strong physical basis of double-porosity models allows parameter calibration by means of independent micro-structural and phenomenological information. Note that only the parameters of the exchange function have been calibrated in the benchmark test to obtain the satisfactory results presented in Figs. 3 and 4. The macroscopic parameters were in fact derived from independent experiments, while the microscopic ones were obtained by means of pore size distribution analyses. The double-porosity formulation also naturally allows for the reproduction of the aspects of contaminant diffusion that, within the framework of single-porosity models, have been defined as *complicating issues* (Shackelford and Moore, 2013). According to phenomenological models, used in the design and performance assessment of geosynthetic clay liners, the one-dimensional flux of chemical species *j* across a bentonite barrier in direction *z* is generally described by the following simplified phenomenological equation:

$$j = -\phi D^* \frac{\partial c}{\partial z} \quad (26)$$

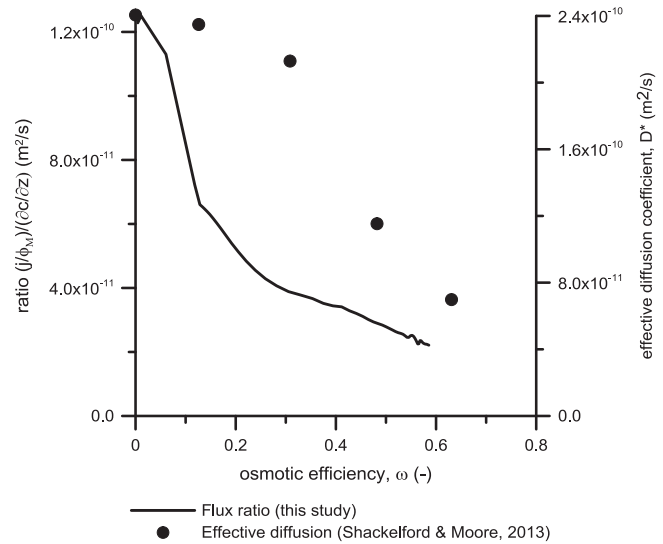


Fig. 9. Effective diffusion coefficient: Model prediction vs. experimental data.

with  $D^*$  being an effective diffusion coefficient which includes the effects of osmotic efficiency, but not porosity dependence. Experimental evidence of the evolution of  $D^*$ , with osmotic efficiency data for a bentonite-based geosynthetic clay liner, is provided in Fig. 9, redrafted from Shackelford and Moore (2013). Effective diffusion values, predicted by the double porosity model, are also shown in Fig. 8. These values have been obtained from the calculated values of solute flux  $j$ , the concentration gradient and macro-porosity during the double-porosity simulation of the test on compacted FEBEX bentonite.

$$D^* = - \frac{(j/\phi_M)}{\left(\frac{\partial c}{\partial z}\right)} \quad (27)$$

Despite the anticipated differences in the magnitude of the effective diffusion parameters, which surely depend on the different structure, density and mineralogy of the two materials, the double-porosity model is proven capable of obtaining the trend in the experimental data.

The very good results obtained with the double-porosity simulations of the diffusion tests performed on reconstituted active clays further suggests that the time-dependent water and salt exchange processes play an important role even in less structured materials, although the definition of micro- and macro-structural domains is different in this case from that of compacted clays.

## Acknowledgments

Financial support from the PRIN research program (Italian Ministry of University and Research, MIUR) “La mitigazione del rischio da frana mediante interventi sostenibili” – contract number 2010SWTCKC\_004 - is gratefully acknowledged.

## References

- Alonso, E.E., Gens, A. & Gehling, W. (1994). Elastoplastic model for unsaturated expansive soils. 3rd Conf. Num. Meth. Geotech. Eng., 11–18.
- Bolt, G.H., 1956. Physico-chemical analysis of the compressibility of pure clays. *Géotechnique* 6 (2), 86–93.
- Bourg, I.C., Sposito, G., Bourg, A.C.M., 2006. Tracer diffusion in compacted, water-saturated bentonite. *Clays Clay Miner.* 54 (3), 363–374. <http://dx.doi.org/10.1346/CCMN.2006.0540307>.
- Bresler, E., 1973. Anion exclusion and coupling effects in non steady transport through unsaturated soils: I. Theory. *Soil Sci. Soc. Am. Proc.* 37, 663–669.
- Brusseau, M.L., Gerstl, Z., Augustijn, D., Rao, P.S.C., 1994. Simulating solute transport in an aggregated soil with the dual-porosity model: measured and optimized parameter values. *J. Hydrol.* 163, 187–193.
- Castellanos, E., Villar, M.V., Romero, E., Lloret, A., Gens, A., 2008. Chemical impact on the hydro-mechanical behavior of high-density FEBEX bentonite. *Phys. Chem. Earth* 33, S516–S526.
- Della Vecchia, G., Jommi, C., Romero, E., 2013. A fully coupled elastic-plastic hydromechanical model for compacted soils accounting for clay activity. *Int. J. Numer. Anal. Methods Geomech.* 37 (5), 503–535.
- Dominijanni, A., Manassero, M., Puma, S., 2013. Coupled chemical-hydraulic-mechanical behaviour of bentonites. *Géotechnique* 63 (3), 191–205.
- Di Maio, C., 1996. Exposure of bentonite to salt solution: osmotic and mechanical effects. *Géotechnique* 46 (4), 695–707.
- ENRESA (2000). FEBEX Project. Full-scale engineered barriers experiment for a deep geological repository for high level radioactive waste in crystalline host rock. Final Report. Technical Publication ENRESA 1/2000. Madrid.
- García-Gutiérrez, M., Cormenzana, J.L., Missana, T., Mingarro, M., 2004. Diffusion coefficients and accessible porosity for HTO and <sup>36</sup>Cl- in compacted FEBEX Bentonite. *Appl. Clay Sci.* 26, 65–73.
- Gens, A., Alonso, E.E., 1992. A framework for the behaviour of unsaturated expansive clays. *Can. Geotech. J.* 29, 1013–1032.
- Gerke, H.H., van Genuchten, M.T., 1993. Evaluation of a first-order water transfer term for variably saturated dual-porosity flow models. *Water Resour. Res.* 29 (4), 1225–1238.
- Guimarães, L.D.N., Gens, A., Sanchez, M., Olivella, S., 2013. A chemo-mechanical constitutive model accounting for cation exchange in expansive clays. *Géotechnique* 63 (3), 221–234.
- Hueckel, T., Kaczmarek, M., Caramuscio, P., 1997. Theoretical assessment of fabric and permeability changes in clays affected by organic contaminants. *Can. Geotech. J.* 34 (4), 588–603.
- Lambe, T.W., 1960. Compacted clay. *Trans. Am. Soc. Civ. Eng.* 125 (Part I), 682–756.
- Loret, B., Hueckel, T., Gajo, A., 2002. Chemo-mechanical coupling in saturated porous media: elastic-plastic behaviour of homoionic expansive clays. *Int. J. Solids Struct.* 39, 2773–2806.
- Lu, N., Olsen, H.W., Likos, W.J., 2004. Appropriate material properties for advective – diffusive solute flux in membrane soil. *J. Geotech. Geoenviron. Eng.* 13, 1341–1346.
- Mitchell, J.K., Soga, 2005. *Fundamentals of Soil Behavior* third ed. John Wiley & Sons. Inc., New York.
- Musso, G., Della Vecchia, G., Romero, E. (2013b). Modelling the coupled chemo-hydro-mechanical behavior of structured active clays on basis of quantitative microstructural information. In *Poromechanics V*, Proceedings of the 5th Biot Conference on Poromechanics, Vienna, Austria. Hellmich, C., Pichler, B. and Adam, D. (Eds.), American Society of Civil Engineers, Reston, Virginia (USA), pp. 1534–1541.
- Musso, G., Della Vecchia, G. (2015). Comparing double porosity and single porosity models for the simulation of coupled chemo-hydro-mechanical behavior of compacted active clays. *Geomechanics from Micro to Macro*. In: *Proceedings of the TC105 ISSMGE International Symposium on Geomechanics from Micro to Macro*, IS-Cambridge, Cambridge, UK. K. Soga, K. Kumar, G. Biscontin, Kuo, M. (Eds.), Taylor & Francis Group, London, pp. 851–856.
- Musso, G., Romero, E., Della Vecchia, G., 2013a. Double structure effects on the chemo-hydro-mechanical behaviour of compacted active clay. *Géotechnique* 63 (3), 206–220.
- Romero, E., Della Vecchia, G., Jommi, C., 2011. An insight into the water retention properties of compacted clayey soils. *Géotechnique* 61 (4), 313–328.
- Santamarina, J.C., Klein, K.A., Fam, M.A., 2001. *Soils and Waves: Particulate Materials Behavior, Characterization and Process Monitoring*. John Wiley & Sons.
- Shackelford, C., Moore, S.M., 2013. Fickian diffusion of radionuclides for engineered containment barriers: diffusion coefficients, porosities, and complicating issues. *Eng. Geol.* 152, 133–147.
- van Genuchten, M. Th, Cleary, R.W., 1982. Movement of solutes in soil: computer-simulated and laboratory results. In: Bolt, G.H. (Ed.), Chapter 10 – Soil Chemistry. B. Physico-Chemical Models. *Developments in Soil Science*. Elsevier Scientific Publishing Company, Amsterdam, pp. 349–386.
- van Olphen, H., 1977. *Clay Colloid Chemistry* third ed. John Wiley & Sons, New York.